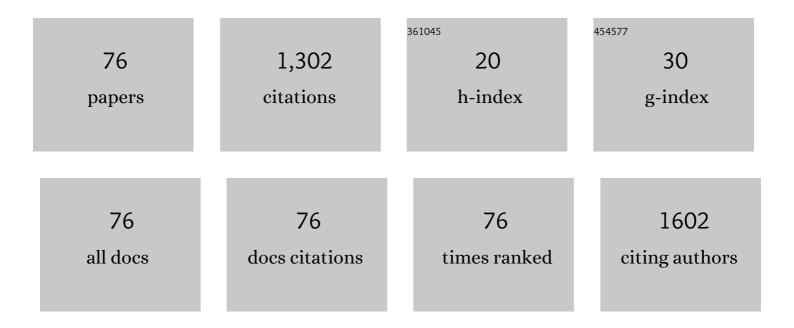
List of Publications by Year in descending order

Source: https://exaly.com/author-pdf/9044947/publications.pdf Version: 2024-02-01



Δοιίο Ρ. Ρλι

#	Article	IF	CITATIONS
1	Self-Powered Broadband Photodetector using Plasmonic Titanium Nitride. ACS Applied Materials & Interfaces, 2016, 8, 4258-4265.	4.0	109
2	Plasmonic Hot Hole Generation by Interband Transition in Gold-Polyaniline. Scientific Reports, 2016, 5, 18276.	1.6	56
3	Observation of sheath modification in laboratory dusty plasma. Physics of Plasmas, 2007, 14, .	0.7	45
4	Optimization of plasma parameters for high rate deposition of titanium nitride films as protective coating on bell-metal by reactive sputtering in cylindrical magnetron device. Applied Surface Science, 2008, 254, 5760-5765.	3.1	45
5	Unraveling the Catalytic and Plasmonic Roles of g-C <sub>3</sub> N <sub>4</sub> Supported Ag and Au Nanoparticles Under Selective Photoexcitation. ACS Sustainable Chemistry and Engineering, 2019, 7, 19295-19302.	3.2	39
6	Pyro-phototronic application in the Au/ZnO interface for the fabrication of a highly responsive ultrafast UV photodetector. Applied Surface Science, 2021, 537, 147893.	3.1	39
7	Highly effective antibiofilm coating of silver–polymer nanocomposite on polymeric medical devices deposited by one step plasma process. Journal of Biomedical Materials Research - Part B Applied Biomaterials, 2014, 102, 1223-1235.	1.6	35
8	Tea-Carbon Dots-Reduced Graphene Oxide: An Efficient Conducting Coating Material for Fabrication of an E-Textile. ACS Sustainable Chemistry and Engineering, 2017, 5, 11645-11651.	3.2	35
9	High photosensitivity with enhanced photoelectrical contribution in hybrid nanocomposite flexible UV photodetector. Organic Electronics, 2014, 15, 2107-2115.	1.4	34
10	An efficient fast response and high-gain solar-blind flexible ultraviolet photodetector employing hybrid geometry. Applied Physics Letters, 2014, 104, 193301.	1.5	33
11	RF-PACVD of water repellent and protective HMDSO coatings on bell metal surfaces: Correlation between discharge parameters and film properties. Applied Surface Science, 2011, 257, 8469-8477.	3.1	32
12	Investigation of sheath properties in Ar/SF6dc discharge plasma. Journal Physics D: Applied Physics, 2003, 36, 645-652.	1.3	29
13	Enhancement of hydrophobicity and tensile strength of muga silk fiber by radiofrequency Ar plasma discharge. Applied Surface Science, 2011, 258, 126-135.	3.1	29
14	TiO2/polyaniline nanocomposite films prepared by magnetron sputtering combined with plasma polymerization process. Applied Surface Science, 2011, 258, 1199-1205.	3.1	27
15	Enhanced light harvesting through Förster resonance energy transfer in polymer–small molecule ternary system. Journal of Materials Chemistry C, 2017, 5, 1136-1148.	2.7	26
16	Development of advanced antimicrobial and sterilized plasma polypropylene grafted muga ( <i>antheraea assama</i> ) silk as suture biomaterial. Biopolymers, 2014, 101, 355-365.	1.2	25
17	Plasmonic Photosensitization of Polyaniline Prepared by a Novel Process for High-Performance Flexible Photodetector. ACS Applied Materials & Interfaces, 2015, 7, 2166-2170.	4.0	25
18	Deposition of nanostructured crystalline and corrosion resistant alumina film on bell metal at low temperature by rf magnetron sputtering. Applied Surface Science, 2009, 255, 7403-7407.	3.1	22

#	Article	IF	CITATIONS
19	Real-time studies of surface roughness development and reticulation mechanism of advanced photoresist materials during plasma processing. Journal of Applied Physics, 2009, 105, 013311.	1.1	21
20	Growth of nanocrystalline TiO2 thin films and crystal anisotropy of anatase phase deposited by direct current reactive magnetron sputtering. Materials Chemistry and Physics, 2013, 139, 979-987.	2.0	21
21	Effect of post-deposition annealing on the growth of nanocrystalline TiO2 thin films and elastic anisotropy of rutile phase at different temperatures. Journal of Alloys and Compounds, 2013, 577, 261-268.	2.8	21
22	Extended Conjugation in Polyaniline Like Structure Prepared by Plasma Polymerization Suitable for Optoelectronic Applications. Plasma Chemistry and Plasma Processing, 2011, 31, 741-754.	1.1	20
23	A hybrid heterojunction with reverse rectifying characteristics fabricated by magnetron sputtered TiO <sub>x</sub> and plasma polymerized aniline structure. Journal Physics D: Applied Physics, 2012, 45, 275401.	1.3	20
24	Studies of radiofrequency plasma deposition of hexamethyldisiloxane films and their thermal stability and corrosion resistance behavior. Vacuum, 2010, 84, 1327-1333.	1.6	19
25	Pulsed PECVD for Lowâ€ŧemperature Growth of Vertically Aligned Carbon Nanotubes. Chemical Vapor Deposition, 2014, 20, 161-169.	1.4	19
26	Observation of instability in presence of E×B flow in a direct current cylindrical magnetron discharge plasma. Physics of Plasmas, 2004, 11, 4719-4726.	0.7	17
27	Study on the influence of nitrogen on titanium nitride in a dc post magnetron sputtering plasma system. Journal Physics D: Applied Physics, 2008, 41, 195205.	1.3	17
28	Plasma process for development of a bulk heterojunction optoelectronic device: A highly sensitive UV detector. Applied Surface Science, 2012, 258, 7897-7906.	3.1	17
29	Biomimetic growth and substrate dependent mechanical properties of bone like apatite nucleated on Ti and magnetron sputtered TiO <sub>2</sub> nanostructure. Journal Physics D: Applied Physics, 2016, 49, 145304.	1.3	17
30	Biomimetic deposition of carbonate apatite and role of carbonate substitution on mechanical properties at nanoscale. Materials Letters, 2016, 185, 387-390.	1.3	17
31	Mechanistic study of ultralow k-compatible carbon dioxide <i>in situ</i> photoresist ashing processes. I. Process performance and influence on ULK material modification. Journal of Vacuum Science and Technology B:Nanotechnology and Microelectronics, 2010, 28, 952-960.	0.6	16
32	Studies of physical and chemical properties of styrene-based plasma polymer films deposited by radiofrequency Ar/styrene glow discharge. Progress in Organic Coatings, 2011, 70, 75-82.	1.9	16
33	Pulsed DC discharge for synthesis of conjugated plasma polymerized aniline thin film. Applied Surface Science, 2012, 259, 691-697.	3.1	15
34	Role of ion energy on growth and optical dispersion of nanocrystalline TiO2 films prepared by magnetron sputtering with ion assistance at the substrate. Applied Surface Science, 2012, 258, 5659-5665.	3.1	14
35	Role of Plasma Parameters on the Conjugated Structure Retention in Polyaniline Thin Film. Plasma Chemistry and Plasma Processing, 2012, 32, 817-832.	1.1	14
36	Low loaded platinum (Pt) based binary catalyst electrode for PEMFC by plasma co-sputtered deposition method. Materials Chemistry and Physics, 2019, 236, 121796.	2.0	14

#	Article	IF	CITATIONS
37	Hot carrier devices using visible and NIR responsive titanium nitride nanostructures with stoichiometry variation. Optical Materials, 2019, 97, 109379.	1.7	14
38	Influence of low energy ion beam on sheath characteristics in plasma. Physics Letters, Section A: General, Atomic and Solid State Physics, 2002, 305, 419-426.	0.9	13
39	Influence of electron beam injection on plasma parameters and sheath in a dc discharge plasma. Journal of Applied Physics, 2003, 94, 6328-6333.	1.1	13
40	lon beam interaction with a potential dip formed in front of an electron-absorbing boundary. Plasma Sources Science and Technology, 2006, 15, 59-63.	1.3	13
41	Effect of oxygen on the characteristics of radio frequency planar magnetron sputtering plasma used for aluminum oxide deposition. Journal of Applied Physics, 2007, 101, 083304.	1.1	13
42	Comparative study of structural and optical properties of pulsed and RF plasma polymerized aniline films. Applied Surface Science, 2014, 313, 286-292.	3.1	13
43	Plasmonic visible-NIR photodetector based on hot electrons extracted from nanostructured titanium nitride. Journal of Applied Physics, 2019, 126, 083108.	1.1	13
44	Effect of impinging ion energy on the substrates during deposition of SiOx films by radiofrequency plasma enhanced chemical vapor deposition process. Thin Solid Films, 2011, 519, 7864-7870.	0.8	12
45	Sheath and potential characteristics in rf magnetron sputtering plasma. Journal of Applied Physics, 2006, 100, 083303.	1.1	11
46	Contradictory ageing behaviour and optical property of iodine doped and H2SO4 doped pulsed DC plasma polymerized aniline thin films. Solid State Sciences, 2013, 24, 71-78.	1.5	11
47	Crystalline rubrene <i>via</i> a novel process and realization of a pyro-phototronic device with a rubrene-based film. Journal of Materials Chemistry C, 2020, 8, 6450-6460.	2.7	11
48	Investigation of the <i>E</i> × <i>B</i> rotation of electrons and related plasma characteristics in a radio frequency magnetron sputtering discharge. Journal Physics D: Applied Physics, 2007, 40, 6865-6872.	1.3	10
49	Interband transition in plasmonic titanium nitride and its contribution towards ZnO based pyro-phototronic application. Materials Chemistry and Physics, 2022, 275, 125290.	2.0	10
50	Role of hydrogen diffusion in temperature-induced transformation of carbon nanostructures deposited on metallic substrates by using a specially designed fused hollow cathode cold atmospheric pressure plasma source. Journal Physics D: Applied Physics, 2017, 50, 155207.	1.3	9
51	Synthesis and characterization of plasma polymerized styrene films by rf discharge. Journal of Physics: Conference Series, 2010, 208, 012104.	0.3	8
52	Effect of <i>E</i> × <i>B</i> electron drift and plasma discharge in dc magnetron sputtering plasma. Chinese Physics B, 2011, 20, 014701.	0.7	8
53	Comparative study of nanocomposites prepared by pulsed and dc sputtering combined with plasma polymerization suitable for photovoltaic device applications. Materials Chemistry and Physics, 2014, 148, 540-547.	2.0	8
54	Atomic level understanding of site-specific interactions in Polyaniline/TiO2 composite. Chemical Physics Letters, 2016, 645, 144-149.	1.2	8

#	Article	IF	CITATIONS
55	Synergistic Effect of Au Interband Transition on Graphene Oxide/ZnO Heterostructure: Experimental Analysis with FDTD Simulation. ACS Omega, 2022, 7, 7662-7674.	1.6	8
56	Characteristics of presheath in multicomponent plasma with negative ions. Physics Letters, Section A: General, Atomic and Solid State Physics, 2004, 333, 102-109.	0.9	7
57	Effect of Radiofrequency Plasma Assisted Grafting of Polypropylene on the Properties of Muga Silk Yarn. Plasma Chemistry and Plasma Processing, 2012, 32, 1293-1306.	1.1	7
58	Enhanced light sensing performance of a hybrid device developed using as-grown vertically aligned multiwalled carbon nanotubes on TCO substrates. RSC Advances, 2014, 4, 46970-46975.	1.7	7
59	Plasma Based Synthesis of Nanomaterials for Development of Plasmon Enhanced Infrared Responsive Optoelectronic Device. Plasma Chemistry and Plasma Processing, 2019, 39, 277-292.	1.1	7
60	Single-Step Preparation of Graphene Oxide Transparent Electrode by PECVD and its Application in a Fast-Response UV-A-Selective Pyrophototronic Device. Journal of Electronic Materials, 2020, 49, 5467-5477.	1.0	7
61	Self-similarity of electrostatic fluctuations in a linear magnetised plasma system. Physics Letters, Section A: General, Atomic and Solid State Physics, 2006, 350, 380-385.	0.9	6
62	Investigations of the hydrophobic and scratch resistance behavior of polystyrene films deposited on bell metal using RF-PACVD process. Applied Surface Science, 2011, 257, 4211-4218.	3.1	6
63	Immobilization of trypsin on plasma prepared Ag/PPAni nanocomposite film for efficient digestion of protein. Materials Science and Engineering C, 2014, 43, 237-242.	3.8	6
64	Investigations on the transformation of vertically aligned CNTs to intramolecular junctions by atmospheric pressure PECVD. Materials Today Communications, 2018, 16, 178-185.	0.9	6
65	A hybrid system for plasmonic and surface polarization induced pyro-phototronic harvesting of light. Optical Materials, 2021, 122, 111733.	1.7	6
66	Fabrication of a heterostructure device with Au/PPani–TiO <sub>2</sub> /ITO configuration and study of device parameters including current conduction mechanism. Journal Physics D: Applied Physics, 2013, 46, 325301.	1.3	5
67	Sheath characteristics in multi-component plasma with negative ions. Pramana - Journal of Physics, 2004, 62, 1091-1098.	0.9	4
68	The influence of RF power and gas pressure on the surface characteristics of aluminium oxide deposited by RF magnetron sputtering plasma. Journal of Physics: Conference Series, 2010, 208, 012102.	0.3	4
69	Enhancement of proton conductivity of sulfonated polystyrene membrane prepared by plasma polymerization process. Bulletin of Materials Science, 2014, 37, 1613-1624.	0.8	4
70	An all metal nitride nanostructure configuration: Study and exploitation in efficient photo-detection. Journal of Alloys and Compounds, 2021, 879, 160460.	2.8	4
71	Mechanistic study of ultralow k-compatible carbon dioxide <i>in situ</i> photoresist ashing processes. II. Interaction with preceding fluorocarbon plasma ultralow k etching processes. Journal of Vacuum Science and Technology B:Nanotechnology and Microelectronics, 2010, 28, 961-967.	0.6	3
72	Pulsed Plasma Assisted Growth of Vertically Aligned Carbon Nanotubes at Low Temperature on Mo Substrate. Plasma Chemistry and Plasma Processing, 2015, 35, 247-257.	1.1	2

#	Article	IF	CITATIONS
73	Plasmon Thin Film Transistor Using Plasma Polymerized Aniline–Rubrene–Gold Nanocomposite in One-Step Process. Plasma Chemistry and Plasma Processing, 2020, 40, 371-386.	1.1	2
74	Microstructural, optical, and dielectric properties of nanocrystalline TiO <sub>2</sub> films prepared via ion-assisted magnetron sputtering. International Journal of Materials Research, 2012, 103, 564-570.	0.1	1
75	One-step grown multi-walled carbon nanotubes with Ni filling and decoration. Journal Physics D: Applied Physics, 2015, 48, 225303.	1.3	1
76	Gold Nanoparticle-Crystalline rubrene hybrid nanocomposite via plasma processing and realization of Plasmon-enhanced organic thin film transistor with high responsivity. Applied Surface Science, 2022, 599, 153883.	3.1	1